A Data-Driven Model of Pedestrian Following and Emergent Crowd Behavior

Kevin Rio and William H. Warren

Abstract Pedestrian following is a common behavior, and may provide a key link between individual locomotion and crowd dynamics. Here, we present a model for following that is motivated by cognitive science and grounded in empirical data. In Experiment 1, we collected data from leader-follower pairs, and showed that a simple speed-matching model is sufficient to account for behavior. In Experiment 2, we manipulated the visual information of a virtual leader, and found that followers respond primarily to changes in visual angle.

Finally, in Experiment 3, we use the speed-matching model to simulate speed coordination in small crowds of four pedestrians. The model performs as well in these small crowds as it did in the leader-follower pairs. This cognitively-inspired, empirically-grounded model can serve as a component in a larger model of crowd dynamics.

Keywords Cognitive science • Data • Dynamics • Experiment • Following

1 Introduction

Crowds are complex systems, made up of individual pedestrians who interact with one another and their environment to exhibit emergent collective behavior [1]. One of the most successful methods for studying crowd behavior is simulation with individual-based models of locomotion [2], such as the social force model [3, 4]. By specifying the local behavior of pedestrians, and the interactions between them, large-scale patterns emerge at the level of the crowd, such as lane formation [3, 5], jamming [6], stop-and-go waves [3, 7], and turbulence [8].

K. Rio (✉) • W.H. Warren

Department of Cognitive, Linguistic, and Psychological Sciences, Brown University, Providence, RI, USA

e-mail: kevin_rio@brown.edu

Existing crowd models stand to benefit from two underutilized sources of information. First, they should take into account findings from cognitive science, which yields results about the human capabilities for perception, action, and cognition that can be used to inspire new models [9, 10], and generate constraints which limit the space of possible models. Second, models should be tested with experimental and observational data. This has been recognized since the earliest work on crowd locomotion [12], but despite recent efforts [13–17], such empirical validation remains uncommon.

To address these concerns, we have adopted a modeling program motivated by cognitive science and grounded in experimental data. We utilize the behavioral dynamics framework [18], which integrates an information-based approach to perception [19] with a dynamical systems approach to action [20, 21]. A full understanding of behavior in this framework consists in specifying how information about the environment is picked up by the agent and used to control action (a *control law*), and a low-dimensional description of the global behavior that arises as a result (a *behavioral strategy*). We use experimental data on human locomotion to test hypotheses about these processes, and to generate models of pedestrian behavior [22, 23].

This paper applies our approach to the case of pedestrian following. Following is a common behavior, and may provide a key link between individual locomotion and crowd dynamics [24]. Successful followers must control their speed to stay behind the leader, and control their heading to stay on course with the leader. Here we focus on speed control. Our goal is to model the behavioral strategy and visual control law governing following in dyads, and then use this model to simulate the emergent behavior of small crowds.

In Experiment 1, we test candidate behavioral strategies against data collected from leader-follower pairs. In Experiment 2, we test candidate sources of visual information against data collected from pedestrians following a leader in virtual reality. In Experiment 3, we extend the model to simulate speed coordination in small crowds.

2   Experiment 1: Behavioral Dynamics of Following

2.1   *Background*

The goal of Experiment 1 was to determine the behavioral strategies used to control pedestrian following. There are a number of candidate strategies, many of which have been studied in the context of car following [25].

Distance   One strategy is for the follower to maintain a preferred distance from the leader. The follower's acceleration $\ddot{x}_f$ t each time step is given by:

$$\ddot{x}_f = c \cdot [\Delta x - \Delta x_0] \tag{1}$$

where Δx is the current distance between the leader and follower, Δx_0 is the preferred distance, and c is a free parameter. Δx_0 might be chosen in various ways. It could be a constant, such as the initial distance between leader and follower, or it could vary with velocity [26, 27]. In the latter case, the preferred distance is equal to:

$$\ddot{x}_f = c \cdot \left[\Delta x - \alpha - \beta \dot{x}_f \right] \tag{2}$$

where $\dot{x}_f$ is the follower's speed and α, β, and c are free parameters.

Speed Another strategy is for the follower to match the speed of the leader. Follower acceleration is given by:

$$\ddot{x}_f = c \cdot \left[\dot{x}_l - \dot{x}_f \right] \tag{3}$$

where $\dot{x}_l$ is the leader's speed and c is a free parameter. An equivalent expression can be written in terms of the relative speed $\Delta \dot{x}$, which is the difference in speed between the leader and follower:

$$\ddot{x}_f = c \cdot [\Delta \dot{x}] \tag{4}$$

One advantage of this strategy is that it does not require a preferred value for distance, like the previous model does. This is an advantage both for the follower (who does not need to store a fixed distance in memory) and for the model (which does not require an additional parameter).

Ratio The GHR model [28] is "perhaps the most well-known model" of car-following [25]. We use a simplified version, which incorporates a ratio of speed and distance, where follower acceleration is given by:

$$\ddot{x}_f(t) = c \cdot \dot{x}_f^M \cdot \frac{\Delta \dot{x}}{\Delta x^L} \tag{5}$$

and c, M, and L are free parameters.

Linear A linear combination of the speed and distance models was proposed in the context of car-following [29]. Again we use a simplified version, which we call the linear model, where follower acceleration is given by:

$$\ddot{x}_f(t) = c_1 [\Delta \dot{x}] + c_2 \left[\Delta x - \alpha - \beta \dot{x}_f \right] \tag{6}$$

where c_1, c_2, α, and β are free parameters.

Thus there are several hypotheses for the behavioral strategy used to control speed during following. The follower could (1) maintain a particular distance, (2) match the speed of the leader, or (3) combine speed and distance information. Experiment 1 was designed to test these strategies against empirical data collected from real leader-follower pairs.

2.2 Methods

Participants 10 students (4 male, 6 female), participated in Experiment 1.

Apparatus Experiment 1 was conducted in the Virtual Environment Navigation Laboratory (VENLab) at Brown University. Participants walked in a 12×12 m area, and wore bicycle helmets to which tracking units were affixed. Head position and orientation were recorded at a sampling rate of 60 Hz by a hybrid inertial-ultrasonic tracking system.

Procedure A confederate acted as the 'leader,' and the participant as the 'follower.' The initial separation was 1 or 3 m. When each trial began, the leader began walking at a comfortable speed in a straight line. After 2, 3, or 5 steps, the leader would speed up, slow down, or remain at the same speed for 3 steps. Finally, the leader would return to his comfortable speed.

Design Experiment 1 had a 2 (initial separation) $\times$ 3 (speed up, slow down, or constant speed) $\times$ 3 (number of steps) factorial design, with 3 trials per condition, for a total of 54 trials per participant. All variables were within-subject, and trials were presented in a random order.

Data Analysis The time-series of leader and follower head position were filtered, using a forward and backward 4th-order low-pass Butterworth filter with a cutoff frequency of 0.6 Hz, to reduce the effects of side-to-side gait oscillations. The filtered position data were differentiated, to produce time-series of leader and follower speed and acceleration.

2.3 Results and Discussion

For each trial, five models were used to simulate follower acceleration in response to the human leader. Root-mean-squared error (RMSE) was used as a measure of goodness of fit for each model and was used to calculate best fit parameters. Pearson's r was used as a second measure of goodness of fit. An optimization algorithm (BFGS Quasi-Newton method [30]) was used to find the set of parameter values that minimized mean RMSE for each model.

Figure 1 shows a plot of the acceleration predicted by each of the five models for a single trial, generated using the best fit parameters.

Table 1 lists mean RMSE and r values for each model.

A one-way ANOVA showed significant differences in RMSE between the models, $F(4,45) = 365.03$, $p < .001$. Post hoc tests using the Bonferroni correction revealed significant differences between all pairwise combinations of models, $p < .01$, except between the speed (0.26, SD = 0.033) and linear (M = 0.25, SD = 0.029) models, which were not significantly different, $p > .05$.

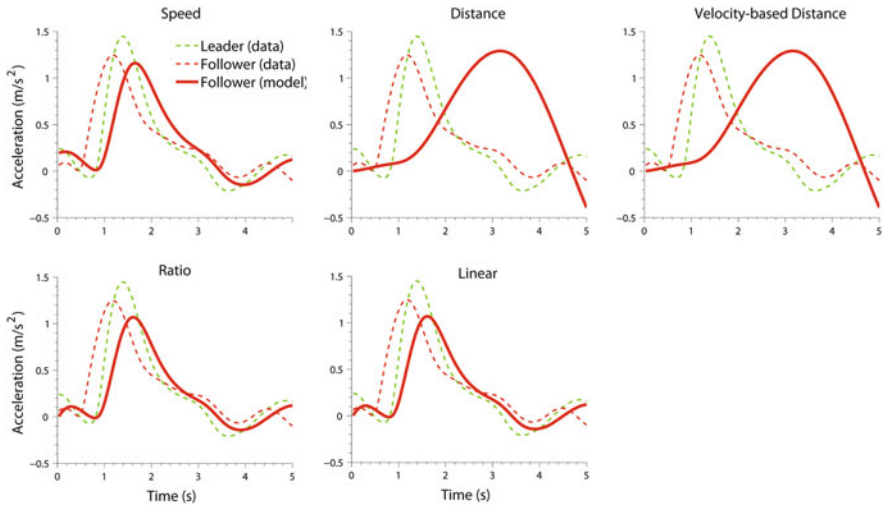**Fig. 1** Time-series of acceleration for a single trial

Table 1 Number of parameters, mean RMSE, and mean r values for five models

Model	# Parameters	Mean RMSE	Mean r
Speed	1	0.26	0.84
Distance	1	0.74	−0.05
Velocity-based distance	2	0.43	0.25
Ratio	3	0.32	0.20
Linear	4	0.25	0.85

These results indicate that the speed model performs as well as the more complicated linear model, and significantly better than the distance, velocity-based distance, and ratio models. A model based on speed provides a better fit to the data than a model based on distance, and adding distance information in the ratio and linear models does not improve performance. Taken together, the results of Experiment 1 support the hypothesis that pedestrian followers rely on a simple strategy of matching the leader's speed.

Several factors constrained followers' behavior in Experiment 1, which could limit the generalizability of our model. First, trials were fairly short, lasting only about 8 s. It is possible that followers adopt a different behavioral strategy when following for longer durations. Second, followers started fairly close to the leader; at longer initial separations, distance information may play a role in addition to or instead of speed information. Despite these constraints, our model is useful because it performs well in the situation that is most relevant to everyday locomotion, following behind a nearby leader, and is robust to changes in initial separation.

3 Experiment 2: Visual Information for Following

3.1 Background

The behavioral strategies described in Experiment 1 are defined in terms of real-world variables, like speed and distance. But observers do not have direct access to these real-world variables; instead, they must rely on information in the optic array. The goal of Experiment 2 was to determine which source(s) of information followers use to control behavior. There are a number of candidate sources; following previous work [31–34], we focus on two of these sources: binocular disparity and visual angle.

Visual Angle The visual angle of the leader has been used to model car-following [35]. The leader's visual angle, α, is a function of the distance between leader and follower, Δx, and the leader's diameter, d. Assuming the leader's height is constant, visual angle depends only on the distance between leader and follower, so maintaining a constant distance behind the leader (a behavioral strategy) is consistent with keeping the leader at a constant visual angle. The change in visual angle, $\dot{\alpha}$, is a function of the relative speed (and distance) between the leader and follower, so a constant relative speed can be achieved by nulling changes in the leader's visual angle.

Binocular Disparity These strategies can also be implemented using binocular disparity. Binocular disparity refers to the difference in retinal images that result from the eyes' horizontal separation; it is a function of an object's distance from an observer. Followers can maintain a constant distance by keeping the relative disparity between the leader and the background constant, and maintain a constant relative speed by nulling changes in disparity.

When the leader speeds up relative to the follower, its binocular disparity increases and its visual angle decreases. Typically, these variables are coupled, but in virtual reality, they can be dissociated [35]. Disparity and visual angle can be manipulated independently by expanding or shrinking the leader as it moves relative to the follower. If followers rely on only one variable, they should speed up when it specifies an increase in leader speed (or vice versa), but not be affected by changes in the other. Conversely, if they rely on both variables, behavior will be sensitive to changes in either one.

Thus there are several hypotheses for the optical information that could be used to control real-world variables like relative speed. The follower could (1) use visual angle, (2) use binocular disparity, or (3) use some combination of the two. Experiment 2 was designed to test these hypotheses against experimental data collected from real pedestrians following a virtual leader.
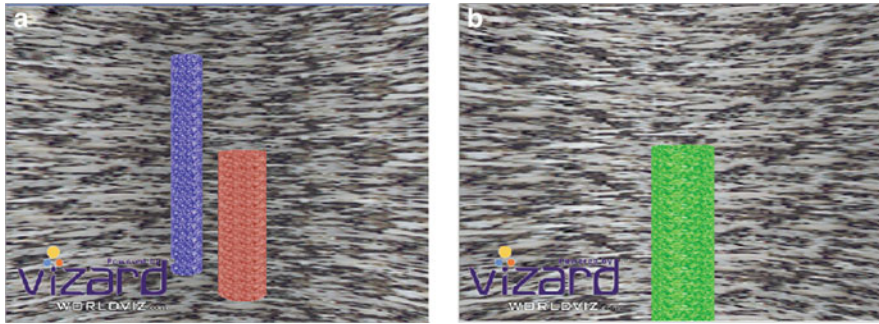
Fig. 2 First-person view of the virtual display used in Experiment 2. **(a)** The blue 'home' pole; participants walk into it and face the red 'target' pole. **(b)** The 'target' pole during following; the pole turns green and begins moving after a button press by the participant

3.2 Methods

Participants 12 students (6 male, 6 female), participated in Experiment 2.

Apparatus Experiment 2 was conducted in the VENLab. Participants walked in a 12×12 m area while viewing a virtual environment through a head-mounted display (HMD), which provided stereoscopic viewing with a 68° horizontal × 53° vertical field of view with a resolution of $1,280 \times 1,240$ pixels. Displays were generated at a frame rate of 60 fps using the Vizard software package. Head position and orientation were tracked as in Experiment 1, and used to update the display with a latency of approximately 50 ms (three frames).

Displays The virtual environment was sparse, consisting of a vertical cylindrical surface (radius 20 m) mapped with a grayscale granite texture and no ground plane. A blue home pole (radius 0.2 m, height 3.0 m) with a granite texture appeared at the center of the environment, and a green/red target pole (radius 0.3 m, height 1.7 m) appeared 1 m away. Figure 2 shows a first-person view of the virtual environment.

Procedure Before each trial, participants stood at the home pole and faced the target pole. To begin a trial, participants pushed a handheld button, which caused the target pole to turn green. After 1 s, the target pole began moving through the environment horizontally in depth. For the first 0.5 s of the trial, the pole's velocity increased linearly from 0 to 0.8 m/s. Its speed then remained constant for a variable amount of time (M = 2.5 s, SD = 1 s) until a "manipulation" lasting 3 s changed the visual angle and/or the binocular disparity of the target pole. Participants were instructed to follow the pole; no further instructions were given regarding speed or distance.

Binocular disparity was manipulated by having the pole speed up (to 1.2 m/s) or slow down (to 0.4 m/s), or by having it remain the same speed. Visual angle was manipulated by having the pole expand or shrink such that its visual angle

Table 2 List of conditions for Experiment 2

		Visual angle-specified speed (m/s)		
		0.4	0.8	1.2
Disparity-specified speed (m/s)	0.4	Speed up	Disparity manipulation	Conflict
	0.8	Visual angle manipulation	Constant speed	Visual angle manipulation
	1.2	Conflict	Disparity manipulation	Slow down

was consistent with a pole of the original dimensions (radius 0.6 m, height 1.6 m) moving at 0.4, 0.8, or 1.2 m/s. There were three possible manipulations for each cue, which were fully crossed, for a total of nine manipulations. These conditions are shown in Table 2.

Design Experiment 2 had a 3 (disparity) × 3 (visual angle) factorial design, with 8 trials per condition, for a total of 72 trials per participant. All variables were within-subject, and trials were presented in a random order.

Data Analysis Data was filtered and differentiated as in Experiment 1. For each trial, the mean change in the follower's speed (ΔSpeed, or ΔS) during the visual manipulation was computed by subtracting the participant's mean speed in the 2 s interval from 1 s after the onset of the visual manipulation until its offset from their mean speed in the 2 s interval prior to the manipulation. A positive value specifies that the participant sped up during the manipulation. The mean of these ΔS values, averaged across participants, was used as a measure of behavioral response to each manipulation.

3.3 Results and Discussion

The mean ΔSpeed values are shown in Fig. 3. In the visual angle manipulation, participants speed up (ΔS = 0.13 m/s) relative to baseline (ΔS = −0.01 m/s) when visual angle-specified speed increases, and slow down (ΔS = −0.29 m/s) when visual angle-specified speed decreases. This is not the case for the binocular disparity manipulations, however. There is no significant difference in speed when disparity-specified speed increases (ΔS = −0.04 m/s) or decreases (ΔS = −0.09 m/s) relative to baseline.

This same pattern of results is observed, regardless of whether a single cue was manipulated, both cues were congruent, or the cues were in conflict. When visual angle decreases, for example, mean changes in speed do not differ when disparity increases (ΔS = 0.10 m/s), remains constant (ΔS = 0.12 m/s), or decreases (ΔS = 0.17 m/s). A two-way ANOVA showed a significant main effect of

Fig. 3 Mean ΔSpeed values for the nine visual manipulation conditions, across trials and participants. Positive values represent an increase in walking speed as a result of the manipulation; negative values represent a decrease. Error bars represent standard error of the mean
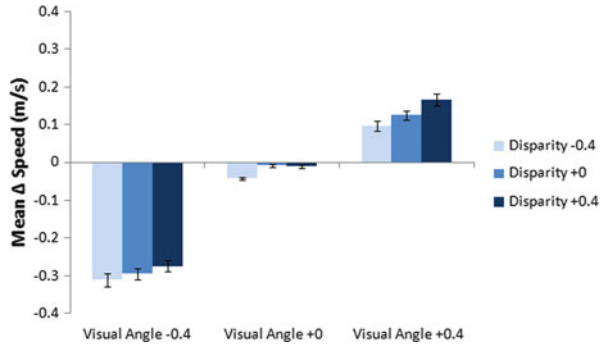
visual angle, $F_{(2,81)} = 99.55$, $p < .001$, no main effect of disparity, $F_{(2,81)} = 1.14$, $p > .05$, and no interaction, $F_{(4,81)} = .12$, $p > .05$.

These results suggest that visual angle is the primary source of optical information used to regulate human following. The follower's speed changed significantly only when visual angle was manipulated. Changes in disparity did not result in changes in speed. Even in the conflict condition, the behavioral response was always in the same direction as visual angle, and it was the same magnitude as when disparity was congruent or unchanged. This indicates that these two cues are not combined.

It is important to note that only a limited range of values were tested. We examined visual angle and disparity manipulations which corresponded to speed changes of $+ 0.4$ m/s and lasted 3 s. This created a rather large conflict between the two sources of information, such that the visual system may have 'vetoed' [37] the weaker disparity information rather than integrating it with visual angle. However, the tested values are realistic for the case of pedestrian following, so the results indicate that following is primarily controlled by changes in visual angle.

4 Experiment 3: Following in Small Crowds

4.1 Background

So far, we have provided evidence that pedestrian followers match leader speed (Experiment 1) by nulling changes in visual angle (Experiment 2). In Experiment 3, our goal is to use this model to predict the acceleration of pedestrians in small crowds. Specifically, we ask whether pedestrians follow neighbors in a crowd as they do in dyads.

Small crowds represent a vital link between studies of individual locomotion and larger crowds of hundreds or thousands of pedestrians, and have been the subject of observational [38] and experimental [16, 39–41] investigations. Studying small

crowds permits experimental control, which can be difficult in large crowds (see [40]), and allows for a richer set of interactions between pedestrians than studies of individuals or dyads.

We collected data from small crowds of four pedestrians walking toward a common goal. In a preliminary analysis [42], we found evidence for collective behavior, such as the adoption of a common speed and the appearance of a preferred density. Here, we extend this analysis by applying the speed-matching model derived from Experiments 1 and 2.

4.2 Methods

Participants 20 students (8 male, 12 female) participated in Experiment 3.

Apparatus Experiment 3 used the same apparatus as Experiment 1.

Procedure An overhead view of the experimental geometry is shown in Fig. 4. Before each trial, participants were assigned to individual starting positions, at the corners of a square, with lengths of 0.5, 1.0, 1.5, or 2.5 m on a side. This resulted in four initial densities. Participants were instructed to walk toward one of three goal posts (radius 0.15 m, height 2, 2 m apart).

To begin each trial, an experimenter verbally instructed the participants to begin walking forward ("Start!"). When the last participant traveled 1 m from the starting positions, an experimenter verbally instructed the participants toward one of the three goals (e.g. "Three!"). Participants walked toward the goal and touched it with their hand. An experimenter signaled that the trial was over ("Stop!"), and starting positions were assigned for the next trial.

Design Experiment 3 had a 4 (density) $\times$ 3 (goal position) factorial design, with 8 trials per condition, for a total of 96 trials per group (480 total). All variables were within-group, and trials were presented in a random order.

Data Analysis Data was filtered and differentiated as in Experiment 1.

4.3 Results and Discussion

The present analysis focuses on the goal 2 condition, in which the goal was located directly ahead of the starting positions. Thus, the primary mode of coordination between participants was in speed, rather than heading. Participants can be divided into six pairs, which represent front-back, side-side, and diagonal couplings. Correlations between the time-series of speed for all six pairs are high ($M = 0.77$, $SD = 0.23$), providing evidence for coordination.
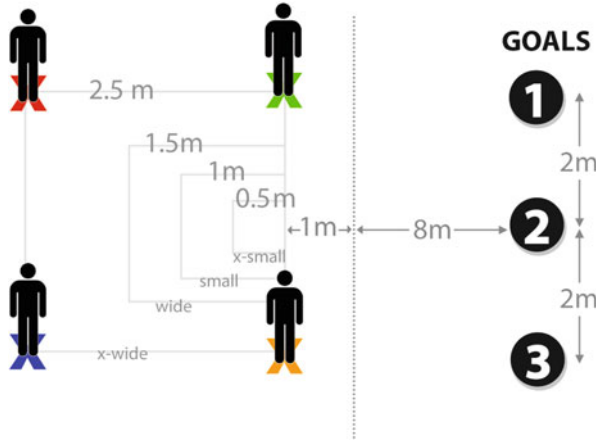
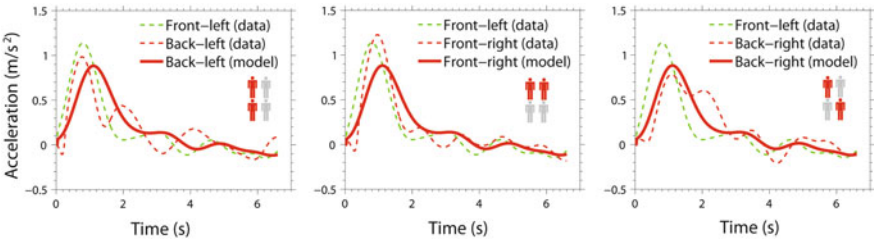**Fig. 4** Overhead view of Experiment 3 geometry (not to scale)

Fig. 5 Time-series of acceleration (data and model predictions) for a single trial

The speed-matching model derived from Experiments 1 and 2 was used to predict the acceleration of one participant as a function of another's speed. Front-back and diagonal couplings are assumed to be unidirectional, so the participant in front always served as the 'leader' in the model. Side-side couplings are bidirectional, so two simulations were performed and then averaged, with each participant serving as 'leader' and 'follower,' respectively. The speed-matching model performs as well on the front-back pairs (RMSE $= 0.19$ m/s^2, r $= 0.78$) as on the following data from Experiment 1 (RMSE $= 0.26$ m/s^2, r $= 0.84$) using fixed parameters. This shows that our model generalizes to speed coordination in small crowds. Figure 5 shows a plot of observed and predicted follower acceleration for 3 pairs of pedestrians.

Some caution is warranted in interpreting these findings. First, Experiment 3 included an acceleration at the beginning, rather than a speed change in the middle of the trial, as in Experiment 1. This may have reduced variability in speed, leading to improved model performance. Second, the common Go signal may have produced spurious correlations. Despite these limitations, the model presented here represents an important first step in linking individual locomotion with coordinated locomotion in small crowds.

5   Conclusion

Empirical validation is necessary for the development of realistic models of human crowds. Here, we have presented a data-driven model of speed control in pedestrian following, derived from experimental results on the behavioral strategy (Experiment 1) and visual information (Experiment 2) in leader-follower pairs. We then showed that this model generalizes to more complex scenarios involving small crowds (Experiment 3) with fixed parameters. Pedestrians appear to follow neighbors in crowds just as they do in dyads.

This model exemplifies our bottom-up approach to understanding crowd dynamics as an emergent phenomenon. By deriving empirical models of local pedestrian interactions, we seek to account for crowd behavior while producing realistic individual trajectories. The speed-matching component generates a form of spatiotemporal coordination that many models [2] have taken to be a primary behavior, along with attraction and repulsion. Our group has developed similar data-driven components for steering and obstacle avoidance based on human experiments [22, 23]. Taken together, they are building toward a model of crowd dynamics in which each individual component has been derived from data, rather than postulated ad hoc [43].

References

 1. Goldstone, R.L., Gureckis, T.M.: Collective Behavior. Top. Cogn. Sci. 1(3), 412–438 (2009)
 2. Reynolds, C.W.: Flocks, Herds, and Schools: A Distributed Behavioral Model. Comp. Graph. 21(4), 25–34 (1987)
 3. Helbing, D., Molnár., P.: Social Force Model for Pedestrian Dynamics. Phys. Rev. E. 51(5), 4282–4286 (1995)
 4. Helbing, D., Farkas, I., Vicsek, T.: Simulating Dynamical Features of Escape Panic. Nature 407(6803), 487–490 (2000)
 5. Piccoli, B., Tosin, A.: Pedestrian Flows in Bounded Domains with Obstacles. Continuum Mech. Therm. 21(2), 85–107 (2009)
 6. Muramatsu, M., Irie, T., Nagatani, T.: Jamming Transition in Pedestrian Counter Flow. Physica A, 267(3–4), 487–498 (1999)
 7. Portz, A., Seyfried, A.: Modeling Stop-and-Go Waves in Pedestrian Dynamics. In: Wryzkowski, R., Dongarra, J., Karczewski, K., Wasniewski, J. (eds.) LNCS, vol. 6068, pp. 561–568. Springer, Heidelberg (2010)
 8. Yu, W., Johansson, A.: Modeling Crowd Turbulence by Many-Particle Simulations. Phys. Rev. E 76(4), 046105 (2007)
 9. Ondřej, J., Pettré, J., Olivier, A.-H., Donikian, S.: A Synthetic-Vision Based Steering Approach for Crowd Simulation. ACM T. Graphic. 29(4), 123 (2010)
10. Moussaïd, M., Helbing, D., Theraulaz, G.: How Simple Rules Determine Pedestrian Behavior and Crowd Disasters. Proc. Natl. Acad. Sci. USA 108(17), 6884–6888 (2011)
11. Lakoba, T.I., Kaup, D.J., Finkelstein, N.M.: Modifications of the Helbing-Molnár-Farkas-Vicsek Social Force Model for Pedestrian Evolution. Simulation 81(5), 339–352 (2005)
12. Henderson, L.F.: The Statistics of Crowd Fluids. Nature 229, 381–383 (1971)

13. Kretz, T., Grünebohm, A., Schreckenberg, M.: Experimental Study of Pedestrian Flow through a Bottleneck. J. Stat. Mech. P10014 (2006)
14. Moussaïd, M., Helbing, D., Garnier, S., Johansson. A., Combe, M., Theraulaz, G.: Experimental Study of the Behavioral Mechanisms Underlying Self-Organization in Human Crowds. P. Roy. Soc. B. 276(1688), 2755–2762 (2009)
15. Robin, T., Antonini, G., Bierlaire, M., Cruz, J.: Specification, Estimation, and Validation of a Pedestrian Walking Behavior Model. Transport. Res. B. 43(1), 36–56 (2009)
16. Moussaïd, M., Perozo, N., Garnier, S., Helbing, D., Theraulaz, G.: The Walking Behaviour of Pedestrian Social Groups and Its Impact on Crowd Dynamics. PLoS One 5(4), e10047 (2010)
17. Schadschneider, A., Seyfried, A.: Empirical Results for Pedestrian Dynamics and Their Implications for Modeling. Netw. Heterog. Media 6(3), 545–560 (2011)
18. Warren, W.H.: The Dynamics of Perception and Action. Psychol. Rev. 113(2), 358–389 (2006)
19. Gibson, J.J.: The Ecological Approach to Visual Perception. Psychology Press, New York (1979)
20. Kugler, P., Turvey, M.: Information, Natural Law, and the Self-Assembly of Rhythmic Movement: Resources for Ecological Psychology. Erlbaum, Hillsdale (1987)
21. Kelso, S.: Dynamic Patterns: The Self-Organization of Brain and Behavior (Complex Adaptive Systems). The MIT Press, Cambridge (1995)
22. Fajen, B.R., Warren, W.H.: Behavioral Dynamics of Steering, Obstacle Avoidance, and Route Selection. J. Exp. Psychol. Human 29(2), 343–362 (2003)
23. Fajen, B.R., Warren, W.H.: Behavioral Dynamics of Intercepting a Moving Target. Exp. Brain Res. 180(2), 303–319 (2007)
24. Li, T.-Y., Jeng, Y.-J., Chang, S.-I.: Simulating Virtual Human Crowds with a Leader-Follower Model. In: Proceedings of the Fourteenth Conference on Computer Animation, pp. 93–102 (2001)
25. Brackstone, M., McDonald, M.: Car-Following: A Historical Review. Transport. Res. F. 2(4), 181–196 (1999)
26. Pipes, L.A.: An Operational Analysis of Traffic Dynamics. J. Appl. Phys. 24(3), 274 (1953)
27. Herman, R., Montroll, E.W., Potts, R.B., Rothery, R.W.: Traffic Dynamics: Analysis of Stability in Car-Following. Oper. Res. 7(1), 86–106 (1959)
28. Gazis, D.C., Herman, R., Rothery, R.W.: Nonlinear Follow-The-Leader Models of Traffic Flow. Oper. Res. 9(4), 545–567 (1961)
29. Helly, W.: Simulation of Bottlenecks in Single Lane Traffic Flow. In: Proceedings of the Symposium on Theory of Traffic Flow, pp. 207–238. Elsevier, New York (1959)
30. Fletcher, R.: Practical Methods of Optimization. Wiley, Hoboken (2000)
31. Regan, D., Beverley, K.I.: Binocular and Monocular Stimuli for Motion in Depth: Changing-Disparity and Changing-Size Feed the Same Motion in Depth Stage. Vision Res. 19, 1331–1342 (1979)
32. Heuer, H.: Estimates of Time-to-Contact Based on Changing Size and Changing Target Vergence. Perception 22(5), 549–563 (1993)
33. Gray, R., Regan, D.: Accuracy of Estimating Time To Collision Using Binocular and Monocular Information. Vision Res. 38, 499–512 (1997)
34. Rushton, S.K., Wann, J.P.: Weighted Combination of Size and Disparity: A Computational Model for Timing a Ball Catch. Nat. Neurosci. 2(2), 186–190 (1999)
35. Anderson, G.J., Sauer, C.W.: Optical Information for Car Following: The Driving by Visual Angle (DVA) Model. Hum. Factors 49(5), 878–896.
36. Tarr, M.J., Warren, W.H.: Virtual Reality in Behavioral Neuroscience and Beyond. Nat. Neurosci. 5, 1089–1092 (2002)
37. Bülthoff, H.H., Mallot, H.A.: Integration of Depth Modules: Stereo and Shading. J. Opt. Soc. Am. A 5(10), 1749–1758 (1988)
38. Costa, M.: Interpersonal Distances in Group Walking. J. Nonverbal Behav. 34(1), 15–26 (2010)
39. Dyer, J.R.G., Johansson, A., Helbing, D., Couzin, I.D., Krause, J.: Leadership, Consensus Decision Making and Collective Behaviour in Humans. Phil. Trans. R. Soc. B. 364(1518), 781–789 (2009)

40. Dyer, J.R.G., Ioannou, C.C., Morrell, L.J., Croft, D.P., Couzin, I.D., Waters, D.A., Krause, J.: Consensus Decision Making in Human Crowds. Anim. Behav. 75(2), 461–470 (2008)
41. Faria, J.J., Dyer, J.R.G., Tosh, C.R., Krause, J.: Leadership and Social Information Use in Human Crowds. Anim. Behav. 79(4), 895–901 (2010)
42. Bonneaud, S., Rio, K., Chevaillier, P., Warren, W.H.: Accounting for Patterns of Collective Behavior in Crowd Locomotor Dynamics for Realistic Simulations. In: Pan, Z., Cheok, A.D., Müller, W., Chang, M., Zhang, M. (eds.) Transactions on Edutainment VIII, LNCS, vol. 7145, pp. 1–12. Springer, Heidelberg (2012)
43. Bonneaud, S., Warren, W.H.: A Behavioral Dynamics Approach to Modeling Realistic Pedestrian Behavior. In: Weidmann, U., Kirsch, U., Puffe, E., Weidmann, M. (eds.) Pedestrian and Evacuation Dynamics. Springer, Heidelberg (2012)